

Delayed excitations induce polymer looping and coherent motion

Andriy Goychuk,^{1,*} Deepti Kannan,² and Mehran Kardar^{2,†}

¹*Institute for Medical Engineering and Science, Massachusetts Institute of Technology, Cambridge, MA 02139, United States*

²*Department of Physics, Massachusetts Institute of Technology, Cambridge, MA 02139, United States*

(Dated: January 29, 2024)

We consider inhomogeneous polymers driven by energy-consuming active processes which encode temporal patterns of athermal kicks. We find that such temporal excitation programs, propagated by tension along the polymer, can effectively couple distinct polymer loci. Consequently, distant loci exhibit correlated motions that fold the polymer into specific conformations, as set by the local actions of the active processes and their distribution along the polymer. Interestingly, active kicks that are canceled out by a time-delayed echo can induce strong compaction of the active polymer.

The biological function of a polymer is tightly connected to its conformational statistics. Longstanding research has illuminated the mechanisms of sequence-controlled polymer folding near thermal equilibrium [1–6]. In such passive systems, the entropic price for folding is paid by monomer-solvent interactions [7–9] and by monomer-monomer interactions, which can encode complex potential landscapes [1, 5]. Similar ideas have been successfully applied to the folding of chromatin, a large heteropolymer consisting of genomic DNA and associated proteins [10]. However, chromatin also shows features of active systems, where nonequilibrium fluctuations [11] and coherent motion [12–14] emerge only in presence of adenosine triphosphate (ATP).

ATP fuels molecular motor activity and biochemical reactions among chromatin-associated proteins [15–17]. For example, SMC complexes [16] share features with other active biochemical systems [18] by cycling between an ADP-bound and an ATP-bound state. Such rapid switching in conformation, interactome and biochemical affinity of chromatin-associated proteins suggests that chromatin potential landscapes actively fluctuate. On a coarse-grained level, these chemically fueled fluctuations can be viewed as local excitations which kick the polymer out of thermal equilibrium. The active kicks at different loci will vary in magnitude and could even show sequence-specific correlations, if driven by long-ranged bulk protein concentration or electrostatic potential gradients [19].

Active processes can elicit polymer folding [19], but cannot be discerned from passive coupling of distant loci via additional Hookean springs [20, 21] based on contact frequency data alone. This structural equivalency allows quasi-equilibrium theories to absorb energy-consuming processes into effective interaction parameters [22, 23]. However, active and passive dynamics are expected to significantly differ [24, 25] in response to ATP [11–14]. To that end, mechanical stress propagation is crucial, because it coordinates the motion of chromosomal loci either via the backbone [26, 27], by chemical interactions among non-neighboring monomers [23, 28–30], or via the surrounding fluid [31, 32]. This suggests local active kicks, for example due to motor activity [27, 31, 33, 34],

or persistent active motion of specific loci [29, 30, 35–49] such as biomolecular condensates [50–54], to have non-local consequences. In contrast to previously studied systems with exponential memory, however, we hypothesize that active force fluctuations, due to binding and unbinding of individual molecular motors [55] or chemical reaction cycles, have specific temporal signatures. Hence, in this letter, we show how an interplay between sequence-specific temporal patterns of excitations and stress propagation can induce correlated motion and folding.

Towards a theoretical framework for such inquiry, we idealize the polymer as a space curve $\mathbf{r}(s, t)$ parametrized by dimensionless material coordinates $s \in [-L/2, L/2]$. Tension propagates along the polymer via lateral stretching modes or via transversal bending modes, as captured by the energetics of an inhomogeneous wormlike chain with Kuhn length b . Assuming dissipative relaxation of the polymer over a microscopic monomer diffusion time τ_b , and active kicks captured through a random velocity field $\boldsymbol{\eta}(s, t)$, the dynamics are described by

$$\tau_b [\partial_t \mathbf{r}(s, t) - \boldsymbol{\eta}(s, t)] = \partial_s [\kappa(s) \partial_s \mathbf{r}(s, t)] - \frac{1}{4} \partial_s^4 \mathbf{r}(s, t). \quad (1)$$

In the limit of uniform activity and $\kappa(s) = \kappa = 1$, the above wormlike chain has steady-state tangent-tangent correlations decaying as $\langle \boldsymbol{\tau}(s, t) \cdot \boldsymbol{\tau}(s', t) \rangle = e^{-|s-s'|/l_p}$, with $\boldsymbol{\tau}(s, t) := b^{-1} \partial_s \mathbf{r}(s, t)$, and dimensionless persistence $l_p = 1/\sqrt{4\kappa}$ along the sequence. In the presence of nonuniform activity, we employ a spatially varying $\kappa(s)$ to enforce an ensemble-averaged and hence weak constraint of local inextensibility, $\langle |\boldsymbol{\tau}(s, t)|^2 \rangle = 1$. Such weak length constraints are certainly different from strongly enforcing inextensibility on the level of individual trajectories, for example, through elastic constraints, which are known to qualitatively affect tension propagation [56]. These limitations notwithstanding, we expect that our simplified theory can provide insights into the folding and dynamics of polymers driven by temporal patterns of excitations. In the following, for convenience and clarity of these ideas, the main text presents analytic theory in the limit of continuous polymers, while figures show numeric evaluations of the analytic theory for discrete chains as described in the Supplemental Material (SM) [57].

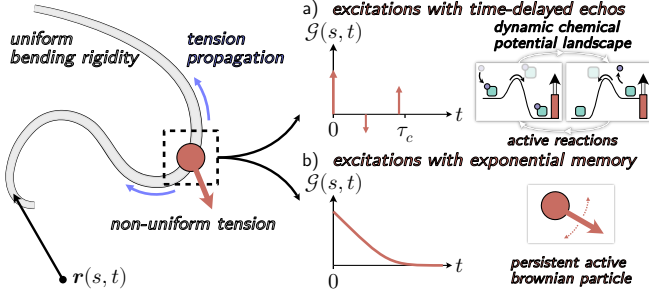


FIG. 1. Sketch of an active semiflexible polymer. Active processes generate excitations, which propagate along the polymer backbone. A non-uniform profile of activity leads to non-uniform line tension, which maintains chain inextensibility. In the present work, we consider two types of excitations: a) Time-delayed echos of past kicks at the same location, such as binding followed by unbinding events. b) Exponentially correlated kicks by persistent self-propelling particles.

To describe temporal patterns of active kicks, we introduce a scalar memory kernel $\mathcal{G}(s, t)$ with characteristic time τ_c , and construct non-Markovian excitations

$$\boldsymbol{\eta}(s, t) = \sqrt{\frac{2b^2}{\tau_b}} \lim_{\varepsilon \rightarrow 0} \int_{-\infty}^{t+\varepsilon} d\tau \left[\frac{\mathcal{G}(s, t-\tau)}{\delta(t-\tau)} \right] \cdot \left[\begin{array}{c} \gamma^a(s, \tau) \\ \gamma^p(s, \tau) \end{array} \right], \quad (2)$$

whose active (a), and passive (p), contributions are seeded by Gaussian noises $\gamma^{a/p}(s, t)$ with zero mean. In the simplest scenario, both contributions have the same characteristic length scale, $\langle \gamma^\alpha(s, t) \cdot \gamma^\beta(s', t') \rangle = \delta_{\alpha\beta} / (2l_e) e^{-|s-s'|/l_e} \delta(t-t')$. The ratio l_e/l_p between the correlation length of the excitations and the polymer is, as explained in this article, a key parameter. In the limit $l_e \rightarrow 0$, excitations are independent along the sequence, while a finite l_e indicates that nearby loci are typically kicked in similar directions. We only consider cases where the variations in $\mathcal{G}(s, t)$ are smooth over the correlation length of the excitations, $\partial_s \mathcal{G} \ll l_e^{-1} \mathcal{G}$, so the covariance is well approximated by

$$\langle \boldsymbol{\eta}(s, t) \cdot \boldsymbol{\eta}(s', t') \rangle = \frac{2b^2}{\tau_b} \frac{1}{2l_e} e^{-\frac{|s-s'|}{l_e}} \widehat{\mathcal{C}}\left(\frac{s+s'}{2}, t-t'\right), \quad (3a)$$

with

$$\widehat{\mathcal{C}}(s, t) = \delta(t) + \lim_{\varepsilon \rightarrow 0} \int_{-\varepsilon}^{\infty} d\tau \mathcal{G}(s, |t| + \tau) \mathcal{G}(s, \tau). \quad (3b)$$

This quantifies how the covariance of athermal excitations [43] explicitly depends on their temporal patterns. We consider two choices of $\mathcal{G}(s, t)$, one which describes heteropolymers assembled from persistent random walkers [35–48], and one where polymers are subject to timed sequences (temporal program) of excitations [Fig. 1].

Having specified the nature of the excitations, we next analyze Eq. (1) via a Rouse mode decomposition [58], where $\mathbf{r}(s, t) \rightarrow \tilde{\mathbf{r}}_q(t)$ and $\boldsymbol{\eta}(s, t) \rightarrow \tilde{\boldsymbol{\eta}}_q(t)$ indicate Fourier

transforms. We compactify the notation by concatenating all Rouse modes row-wise into a matrix $\mathbf{R}(t)$ with rows $R_{q,\dots}(t) := \tilde{\mathbf{r}}_q(t)$, and analogously define the random velocity mode matrix $\mathbf{H}(t)$ with rows $H_{q,\dots}(t) := \tilde{\boldsymbol{\eta}}_q(t)$. The Fourier-transformed Eq. (1) is solved by

$$\mathbf{R}(t) = \int_{-\infty}^t d\tau e^{-\mathbf{J}(t-\tau)} \cdot \mathbf{H}(\tau), \quad (4)$$

with the response matrix, \mathbf{J} , given by $\tau_b J_{qk} = \frac{1}{L} qk \kappa_{q-k} + \frac{1}{4} q^4 \delta_{qk}$. In principle, one could also consider an additional memory kernel that acts on the backbone velocities, $\partial_t \mathbf{r}(s, t)$, and approximates the viscoelasticity of the surrounding medium [26, 59, 60]. The interplay between the timescales of the system could then lead to further interesting effects. Even in the simpler scenario, however, there is already an interplay between the memory of the excitations and the relaxation time of the polymer.

First, we analyze the dynamics of a polymer subjected to generic excitations with covariance $\mathbf{C}(t-t') := \langle \mathbf{H}(t) \cdot \mathbf{H}^\dagger(t') \rangle$ and characteristic decorrelation time τ_c , so that $\mathbf{C}(\tau) \sim 0$ for $|\tau| > \tau_c$. In the limit of either long timescales, $|t-t'| > \tau_c$, or in steady state, $t=t' \rightarrow \infty$, the memory of the excitations can be effectively integrated out [57], because the polymer has ample time to run through many iterations of its excitation program \mathcal{G} . More specifically, one finds that the polymer dynamics resemble that of a chain where the temporal excitation programs are replaced by couplings between different excitation modes, $\langle \mathbf{H}(t) \cdot \mathbf{H}^\dagger(t') \rangle \approx \mathbf{C}_{\text{eff}} \delta(t-t')$ with

$$\mathbf{C}_{\text{eff}} := \int_0^\infty d\tau \left[\mathbf{C}(\tau) \cdot e^{-\mathbf{J}^\dagger \tau} + e^{-\mathbf{J} \tau} \cdot \mathbf{C}^\dagger(\tau) \right]. \quad (5)$$

The covariance $\mathbf{X}(0) \equiv \langle \mathbf{R}(t) \cdot \mathbf{R}^\dagger(t) \rangle$ of the steady-state distribution of conformations is then implicitly defined by the Lyapunov equation $\mathbf{J} \cdot \mathbf{X}(0) + \mathbf{X}(0) \cdot \mathbf{J}^\dagger = \mathbf{C}_{\text{eff}}$. In the limit that the memory is short-lived, $\tau_c \ll \tau_b$, the polymer fluctuations are well approximated by $\langle \mathbf{R}(t) \cdot \mathbf{R}^\dagger(t') \rangle \approx e^{-\mathbf{J}|t-t'|} \cdot \mathbf{X}(0)$ for $t > t'$. The complementary case where the memory is long-lived, $\tau_c \gtrsim \tau_b$, however, can be only obtained by evaluating the analytical solutions numerically. We next analyze specific models for the response matrix of the polymer, \mathbf{J} , and for the temporal pattern of excitations encoded in $\mathbf{C}(\tau)$.

In the simplest scenario, on length scales much larger than the noise correlation length and the persistence length, $\Delta s \gg \max(l_e, 2l_p)$, tension is expected to propagate predominantly through longitudinal modes. In this limit, it is tempting to approximate $\langle \gamma^\alpha(s, t) \cdot \gamma^\beta(s', t') \rangle \approx \delta_{\alpha\beta} \delta(s-s') \delta(t-t')$, set $\kappa(s) = 1$, and drop the bending term in Eq. (1), leading to $\tau_b J_{qk} \sim q^2 \delta_{qk}$. Transforming Eq. (5) from Fourier space to sequence space, one finds

$$\mathbf{C}_{\text{eff}}(s, s') = \frac{2b^2}{\tau_b} \int_0^\infty d\tau \frac{\widehat{\mathcal{C}}(s, \tau) + \widehat{\mathcal{C}}(s', \tau)}{\sqrt{4\pi\tau/\tau_b}} e^{-\frac{(s-s')^2}{4\tau/\tau_b}}, \quad (6)$$

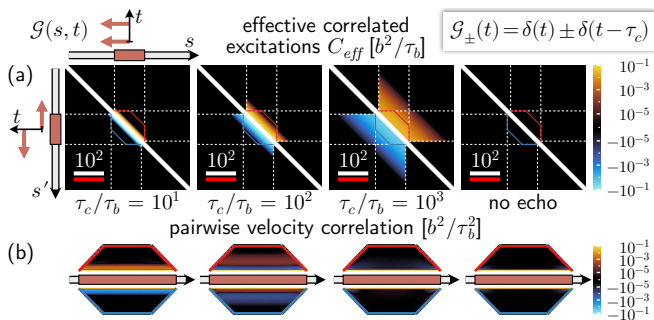


FIG. 2. (a) Local active processes lead to effectively correlated excitations of a discrete 10^3 -mer flexible chain. Red arrows indicate that each active kick in the active region ($\epsilon = 1$ for $s \in$ red segment, delimited by dashed lines) is followed by a time-lagged positive (\mathcal{G}_+ , above diagonal) or negative (\mathcal{G}_- , below diagonal) echo. Scale bars: 10^2 monomers (white) or Kuhn segments (red). (b) Same-time velocity pair correlations, $\langle \mathbf{v}^\delta(s, t) \cdot \mathbf{v}^\delta(s', t) \rangle$ with time discretization $\delta = 0.1\tau_b \ll \tau_c$ shorter than the memory. Red and blue outlines correspond to solid lines in (a). Positive (negative) echos with larger lag time τ_c cause longer-ranged but weaker positive (negative) velocity correlations.

which, as will be illuminated shortly, is a good approximation when $l_e \gg l_p$. Thus, purely local temporal sequences of kicks, which are relayed via the line tension of the polymer backbone, can lead to effective sequence-controlled correlated excitations.

This is illustrated in Fig. 2(a) for a discrete flexible chain subjected to inhomogeneous excitations $\mathcal{G}(s, t) = \sqrt{\epsilon(s)} \mathcal{G}_\pm(t)$ with echos, $\mathcal{G}_\pm(t) = \delta(t) \pm \delta(t - \tau_c)$. Within the lag time τ_c between an active kick and its subsequent echo, forces propagate diffusively across a typical distance $|s - s'| \propto \sqrt{\tau_c/\tau_b}$ [Eq. (6)], effectively coupling the excitations at loci s and s' . Consequently, the locus velocities $\mathbf{v}^\delta(s, t) := [\mathbf{r}(s, t + \delta) - \mathbf{r}(s, t)]/\delta$ also exhibit pairwise correlations which are well approximated by $\langle \mathbf{v}^\delta(s, t) \cdot \mathbf{v}^\delta(s', t) \rangle \approx \delta^{-1} C_{\text{eff}}(s, s')$ for $\tau_c \ll \delta \ll \tau_b$. This approximation fails if the time discretization δ is too fine to integrate out the memory, i.e. when $\delta \ll \tau_c$. Nevertheless, when compared to an explicit evaluation of the pairwise velocity correlations, $C_{\text{eff}}(s, s')$ reasonably predicts which regions show coordinated motion [left two panels in Fig. 2(b)]. As discussed in our prior work [19], because correlated (anticorrelated) excitations imply effective attraction (repulsion) between loci, Eq. (6) also informs about the conformations of the polymer.

To further elucidate the results so far, we now revisit a scenario where the excitations have exponential memory, $\mathcal{G}(s, t) = \sqrt{\epsilon(s)} \tau_c^{-1} e^{-|t|/\tau_c}$, which has been the focus of several theoretical studies [35–47] and reviewed in Ref. [48]. Diffusive propagation of tension through lateral stretching modes [Eq. (6)] leads to

$$C_{\text{eff}}(s, s') = \frac{2b^2}{\tau_b} \left[\delta(s - s') + \frac{\epsilon(s) + \epsilon(s')}{4l_e} e^{-\frac{|s-s'|}{l_e}} \right], \quad (7)$$

with $l_e := \sqrt{\tau_c/\tau_b}$. For a flexible chain, a local increase in activity should then lead to swelling [19, 48]. In contrast, semiflexible active chains can show either contraction or swelling when the average activity is increased [48]. To reconcile these results, we next study the propagation of transversal excitation modes via bending, which we have neglected so far.

Assuming that the activity is large and nearly homogeneous, $\epsilon(s) \gg 1$ and $\partial_s \epsilon(s) \ll l_e^{-1} \epsilon(s)$, the exponential memory can be replaced by memory-less noise of the form $\mathcal{G}(s, t) = \sqrt{\epsilon(s)} \delta(t)$ and a renormalized correlation length $l_e \approx l_c$ in Eq. (3). We determine the local Lagrange multiplier $\kappa(s)$ from the weak constraint $\langle |\boldsymbol{\tau}(s, t)|^2 \rangle = 1$, as shown in the SM [57]. On large length scales (i.e., for long wave modes), the dynamics of the polymer are approximately given by

$$\tau_b [\partial_t \mathbf{r}(s, t) - \boldsymbol{\eta}(s, t)] = \partial_s \left[\left(\frac{1}{\chi} + \frac{2\epsilon(s)}{\chi^{3/2}} \right) \partial_s \mathbf{r}(s, t) \right], \quad (8)$$

where the adjustment $\chi \equiv \chi(l_e)$ rescales the line tension as derived in the SM [57]. The reduction in line tension ensures that the polymer does not contract due to the finite correlation length of the excitations [19]. Figure 3(a) shows the relative weight of the inhomogeneous term in the square brackets of Eq. (8), which for $l_e \gg l_p$ decays as $1/\sqrt{l_e}$. Thus, treating the polymer as an effective Rouse chain is internally consistent [61] if the excitations decorrelate over distances much larger than the Kuhn length [Fig. 3(b)]. Then, large coiled segments (Pincus blobs [62]) experience coherent excitations, primarily leading to agitation of longitudinal modes.

In general, however, Eq. (8) demonstrates that regions with locally increased activity also show an increased tension of the polymer backbone. For cases where the excitations occur on length scales smaller than a Pincus blob, $l_e < 2l_p$, this can qualitatively change the response of the polymer by causing active segments to contract instead of expand [above the diagonal in Fig. 3(b)]. These predictions of continuum theory also apply to discrete semiflexible polymers [below the diagonal in Fig. 3(b)], where the response matrix is described in the SM [57] and in Refs. [63, 64]. Mechanistically, these effects can be traced back to the agitation of transversal bending modes, which inevitably lead to contraction when coupled with a length constraint. Thus, the interplay between features of the athermal excitations and the microscopic mechanics of the polymer can determine if active regions expand ($l_e > 2l_p$) or contract ($l_e < 2l_p$). Extrapolating these results, the persistence time τ_c of active particles can control if semiflexible chains swell or contract [48].

In light of these results, we now revisit the scenario of a wormlike chain subject to temporal sequences of kicks, but this time assume that each excitation has a characteristic size (correlation length) comparable to

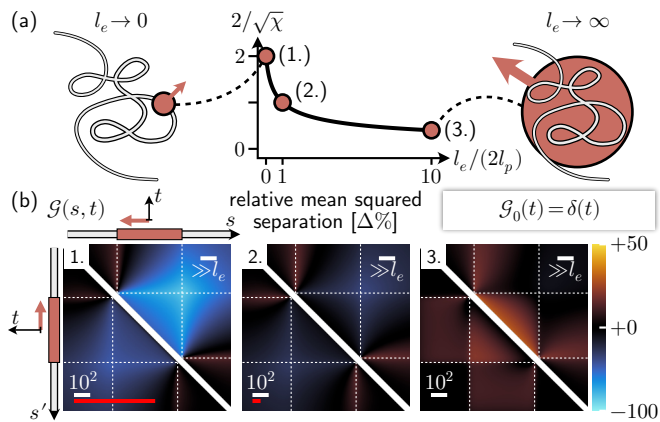


FIG. 3. Response of a semiflexible chain to active processes depends on the noise correlation length l_e . (a) By agitating bending modes, non-uniform activity can induce tension modulations [Eq. (8)], quantified by $2/\sqrt{\chi}$ with control parameter l_e . The limit $l_e \rightarrow \infty$ recovers a flexible chain with uniform tension. (b) Change in pairwise squared separation due to memory-less active kicks in an active region ($\epsilon = 0.5$ for $s \in$ red segment, delimited by dashed lines), compared to a uniform chain. *Above diagonal*: Continuous wormlike chain for different l_e , on arbitrary length scales $\gg l_e$ (scale bar). *Below diagonal*: Discrete semiflexible chain of 10^3 coarse-grained monomers (10^2 , 10^3 , or 10^6 Kuhn lengths) which receive independent kicks. Scale bars: 10^2 monomers (white) or persistence lengths (red). (1.) For $l_e \rightarrow 0$, agitation of bending modes effectively *compacts* the polymer. (2.) For $l_e = 2l_p$, the active polymer resembles an inextensible *flexible* chain. (3.) For $l_e \rightarrow \infty$, the polymer behaves like an extensible flexible chain with agitation of stretching modes.

the length of a Kuhn segment, $l_e \sim 2l_p$. In practice, we approximate this by a discrete semiflexible polymer [57, 63, 64] where each coarse-grained monomer corresponds to a Kuhn length, so that the excitations at different monomers can be assumed independent. As shown in Fig. 4(a), effective bending of active regions [19], combined with the constraint of chain inextensibility, drastically reduces the mean squared separation between the boundaries of the active region, which is indicative of a loop-like state. Compared to a scenario without echos, positive echos deplete contacts within this loop-like domain [above the diagonal in Fig. 4(a)]. Conversely, negative echos enhance contacts and can even induce compaction by almost 100%, reminiscent of a coil-to-globule transition [below the diagonal in Fig. 4(a)]. Negative echos can be viewed as time-delayed analogs of local force dipoles, where the delay originates from stress propagation through internal degrees of freedom. For large molecular motors such as cohesin, for example, the force exerted by one motor head as it extrudes a chromatin loop [65], could propagate along the clamped chromatin loop or the body of the cohesin molecule, and would be echoed by an equal and opposite force at the same locus. Moreover, we expect that time-delayed echos can

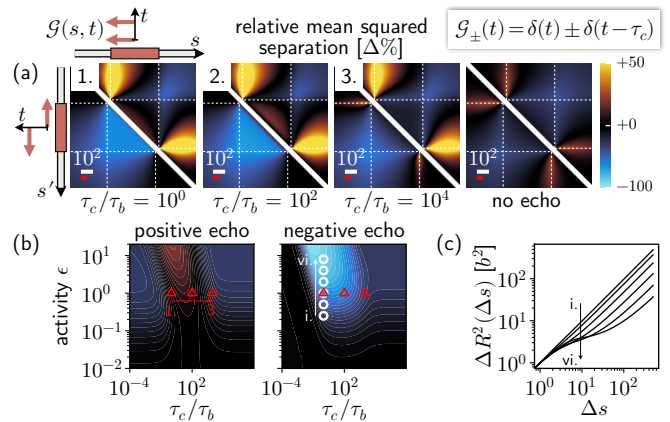


FIG. 4. Response of a discrete 1000-mer semiflexible chain to active processes. (a) Change in pairwise squared separation compared to a uniform chain. Red arrows illustrate that each active kick in the active region ($\epsilon = 1$ for $s \in$ red segment, delimited by dashed lines) is followed by a time-lagged positive (\mathcal{G}_+ , above diagonal) or negative (\mathcal{G}_- , below diagonal) echo. Scale bar: 10^2 monomers (white) or persistence lengths (red). (b) Average change in pairwise separation within the active segment as a function of the activity ϵ and the echo lag time. Time-delayed echos show strongest effect for intermediate time lags ($\tau_c \sim \tau_b$). In the limits $\tau_c \ll \tau_b$ or $\tau_c \gg \tau_b$, excitations become statistically independent. Red triangles correspond to mean squared separation maps in (a). (c) Mean squared distance from the center monomer in a homogeneous semiflexible chain driven by kicks with echos; parameters are indicated by white circles in (b). Negative echos decrease the radius of gyration by introducing a crossover regime where the curves plateau (black arrow).

also arise from interaction forces during local sequences of chemical reactions.

In summary, we have analyzed the conformations and dynamics of a broad class of inhomogeneous active polymers which experience local temporal patterns of excitations. Within this theoretical framework, different segments can vary in activity, persistence time, or even show unique temporal excitation programs. Then, both qualitative features of the excitations (such as, positive or negative echos) and quantitative features (delay times of the echos) determine which regions of the polymer move coherently and how the active segment folds. Moreover, our framework can explain previous theoretical observations of polymer swelling and collapse [37–41, 48] as a competition between a) the polymer persistence length, and b) the typical arc distance that excitations are relayed through tension propagation along the polymer backbone. We hypothesize that such a competition of length scales could be relevant for biopolymers such as chromatin, and could determine if active segments expand or collapse.

We thank Arup K. Chakraborty for engaging in insightful discussions. This work was supported by the National Science Foundation, through the Biophysics of

Nuclear Condensates grant (MCB-2044895). A.G. was also supported by an EMBO Postdoctoral Fellowship (ALTF 259-2022). D.K. was supported by the Graduate Research Fellowship Program under grant No. 2141064. The authors acknowledge the MIT SuperCloud and Lincoln Laboratory Supercomputing Center for providing HPC resources that have contributed to the research results reported within this paper.

* andriy@goychuk.me

† kardar@mit.edu

- [1] J. N. Onuchic, Z. Luthey-Schulten, and P. G. Wolynes, *Annu. Rev. Phys. Chem.* **48**, 545 (1997).
- [2] V. S. Pande, A. Y. Grosberg, and T. Tanaka, *Rev. Mod. Phys.* **72**, 259 (2000).
- [3] E. Shakhnovich, *Chem. Rev.* **106**, 1559 (2006).
- [4] K. A. Dill, S. B. Ozkan, M. S. Shell, and T. R. Weikl, *Annu. Rev. Biophys.* **37**, 289 (2008).
- [5] P. G. Wolynes, *Biochimie* **119**, 218 (2015).
- [6] R. Nassar, G. L. Dignon, R. M. Razban, and K. A. Dill, *J. Mol. Biol.* **433**, 167126 (2021).
- [7] J. L. England and V. S. Pande, *Biophys. J.* **95**, 3391 (2008).
- [8] J. L. England, *Structure* **19**, 967 (2011).
- [9] N. Perunov and J. L. England, *Protein Sci.* **23**, 387 (2014).
- [10] T. Misteli, *Cell* **183**, 28 (2020).
- [11] S. C. Weber, A. J. Spakowitz, and J. A. Theriot, *Proc. Natl. Acad. Sci. U.S.A.* **109**, 7338 (2012).
- [12] A. Zidovska, D. A. Weitz, and T. J. Mitchison, *Proc. Natl. Acad. Sci. U.S.A.* **110**, 15555 (2013).
- [13] M. P. Backlund, R. Joyner, K. Weis, and W. E. Moerner, *Mol. Biol. Cell* **25**, 3619 (2014).
- [14] H. A. Shaban, R. Barth, and K. Bystricky, *Nucleic Acids Res.* **46**, e77 (2018).
- [15] G. J. Narlikar, R. Sundaramoorthy, and T. Owen-Hughes, *Cell* **154**, 490 (2013).
- [16] F. Uhlmann, *Nat. Rev. Mol. Cell Biol.* **17**, 399 (2016).
- [17] M. A. Reid, Z. Dai, and J. W. Locasale, *Nat. Cell Biol.* **19**, 1298 (2017).
- [18] J. Halatek, F. Brauns, and E. Frey, *Philosophical Transactions of the Royal Society B: Biological Sciences* **373**, 20170107 (2018).
- [19] A. Goychuk, D. Kannan, A. K. Chakraborty, and M. Kardar, *Proc. Natl. Acad. Sci. U.S.A.* **120**, e2221726120 (2023).
- [20] G. Le Treut, F. Képès, and H. Orland, *Biophys. J.* **115**, 2286 (2018).
- [21] G. Shi and D. Thirumalai, *Nat. Commun.* **10**, 3894 (2019).
- [22] B. Zhang and P. G. Wolynes, *Biophys. J.* **112**, 427 (2017).
- [23] M. Di Pierro, D. A. Potoyan, P. G. Wolynes, and J. N. Onuchic, *Proc. Natl. Acad. Sci. U.S.A.* **115**, 7753 (2018).
- [24] C. P. Brangwynne, G. H. Koenderink, F. C. MacKintosh, and D. A. Weitz, *Trends in Cell Biology* **19**, 423 (2009).
- [25] F. S. Gnesotto, F. Mura, J. Gladrow, and C. P. Broedersz, *Rep. Prog. Phys.* **81**, 066601 (2018).
- [26] T. J. Lampo, A. S. Kennard, and A. J. Spakowitz, *Biophys. J.* **110**, 338–347 (2016).
- [27] S. Put, T. Sakaue, and C. Vanderzande, *Phys. Rev. E* **99**, 032421 (2019).
- [28] H. Salari, M. Di Stefano, and D. Jost, *Genome Res.* **32**, 28 (2022).
- [29] L. Liu, G. Shi, D. Thirumalai, and C. Hyeon, *PLOS Comput. Biol.* **14**, e1006617 (2018).
- [30] Z. Jiang, Y. Qi, K. Kamat, and B. Zhang, *J. Phys. Chem. B* **126**, 5619 (2022).
- [31] R. Bruinsma, A. Y. Grosberg, Y. Rabin, and A. Zidovska, *Biophys. J.* **106**, 1871 (2014).
- [32] I. Eshghi, A. Zidovska, and A. Y. Grosberg, *Phys. Rev. Lett.* **131**, 048401 (2023).
- [33] D. Saintillan, M. J. Shelley, and A. Zidovska, *Proc. Natl. Acad. Sci. U.S.A.* **115**, 11442 (2018).
- [34] A. Mahajan, W. Yan, A. Zidovska, D. Saintillan, and M. J. Shelley, *Phys. Rev. X* **12**, 041033 (2022).
- [35] A. Ghosh and N. S. Gov, *Biophys. J.* **107**, 1065 (2014).
- [36] A. Kaiser, S. Babel, B. ten Hagen, C. von Ferber, and H. Löwen, *J. Chem. Phys.* **142**, 124905 (2015).
- [37] T. Eisenstecken, G. Gompper, and R. G. Winkler, *Polymers* **8**, 304 (2016).
- [38] T. Eisenstecken, A. Ghavami, A. Mair, G. Gompper, and R. G. Winkler, *AIP Conf. Proc.* **1871**, 050001 (2017).
- [39] S. M. Mousavi, G. Gompper, and R. G. Winkler, *J. Chem. Phys.* **150**, 064913 (2019).
- [40] S. K. Anand and S. P. Singh, *Phys. Rev. E* **101**, 030501 (2020).
- [41] S. Brahmachari, T. Markovich, F. C. MacKintosh, and J. N. Onuchic, *bioRxiv*, 2023.04.23.528410 (2023).
- [42] T. Eisenstecken, G. Gompper, and R. G. Winkler, *J. Chem. Phys.* **146**, 154903 (2017).
- [43] D. Osmanović and Y. Rabin, *Soft Matter* **13**, 963 (2017).
- [44] D. Osmanović, *J. Chem. Phys.* **149**, 164911 (2018).
- [45] T. Saito and T. Sakaue, *Polymers* **11**, 2 (2019).
- [46] A. Ghosh and A. J. Spakowitz, *Phys. Rev. E* **105**, 014415 (2022).
- [47] A. Ghosh and A. J. Spakowitz, *Soft Matter* **18**, 6629–6637 (2022).
- [48] R. G. Winkler and G. Gompper, *J. Chem. Phys.* **153**, 040901 (2020).
- [49] S. Dutta, A. Ghosh, and A. J. Spakowitz, *Soft Matter* **10.1039/D3SM01491F** (2024).
- [50] M. M. Hanczyc, *Phil. Trans. R. Soc. B* **366**, 2885–2893 (2011).
- [51] M. Dindo, A. Bevilacqua, G. Soligo, A. Monti, M. E. Rosti, and P. Laurino, *bioRxiv*, 2023.04.25.538216 (2023).
- [52] E. Jambon-Puillet, A. Testa, C. Lorenz, R. W. Style, A. A. Rebane, and E. R. Dufresne, *bioRxiv* **10.1101/2023.07.18.549556** (2023).
- [53] H. H. Schede, P. Natarajan, A. K. Chakraborty, and K. Shrinivas, *Nature Communications* **14**, 4152 (2023).
- [54] L. Demarchi, A. Goychuk, I. Maryshev, and E. Frey, *Phys. Rev. Lett.* **130**, 128401 (2023).
- [55] F. C. MacKintosh and A. J. Levine, *Phys. Rev. Lett.* **100**, 018104 (2008).
- [56] O. Hallatschek, E. Frey, and K. Kroy, *Phys. Rev. E* **75**, 031905 (2007).
- [57] See Supplemental Material at [URL will be inserted by publisher] for further details.
- [58] P. E. Rouse, *J. Chem. Phys.* **21**, 1272 (1953).
- [59] S. C. Weber, A. J. Spakowitz, and J. A. Theriot, *Phys. Rev. Lett.* **104**, 238102 (2010).
- [60] S. C. Weber, J. A. Theriot, and A. J. Spakowitz, *Phys.*

- Rev. E **82**, 011913 (2010).
- [61] One then recovers the dynamics of a flexible chain by rescaling $s \mapsto \tilde{s}/\chi$ and $t \mapsto \tilde{t}/\chi$ and dropping the tildes.
- [62] M. Rubinstein and R. H. Colby, *Polymer Physics* (Oxford University Press, Oxford, 2003).
- [63] R. G. Winkler, *J. Chem. Phys.* **118**, 2919–2928 (2003).
- [64] A. R. Tejedor, J. R. Tejedor, and J. Ramírez, *J. Chem. Phys.* **157**, 164904 (2022).
- [65] E. J. Banigan and L. A. Mirny, *Curr. Opin. Cell Biol.* **64**, 124 (2020), cell Nucleus.